Macromolecular Research (2024) 32:173–186
https://doi.org/10.1007/s13233-023-00218-6

Online ISSN 2092-7673
Print ISSN 1598-5032

ARTICLE

# Dual stimuli-responsive polymeric prodrug consisting of reversible covalent bonded celastrol for tumor targeted delivery

**Jiangtao Su[1,2,3,4] · Meng Rao[1] · Heshuang Dai[1,2] · Le Cai[1] · Fan Ye[1] · Lu Ye[1] · Yuchen Hu[1,3] · Ban Chen[1,4] · Xiaoxia Guo[1,2,3]**

Received: 30 August 2023 / Revised: 17 October 2023 / Accepted: 19 October 2023 / Published online: 14 November 2023


## Abstract

In this work, pH/GSH-responsive amphiphilic polymeric prodrug (EDA-GLA/CE/2-FPBA) was successfully prepared and could self-assembled into micelles in an aqueous solution. The EDA-GLA/CE/2-FPBA micelles possessed high stability in physiological condition and were pH and GSH sensitive due to the reversible borate ester bonds and disulfide bonds within the prodrug polymer. The structures of the prodrug polymers were characterized by NMR, FTIR, UV–vis spectroscopy. Transmission electron microscopy and dynamic light scattering measurement indicated that the resulting micelles have desirable size distribution and regular spherical shape. Free active Celastrol can be released under low pH and high GSH environment; In vitro cellular uptake and growth inhibition assays suggested that the blank polymer micelles showed good biocompatibility. EDA-GLA/CE/2-FPBA micelles were more efficiently internalized by monolayer tumor cells and demonstrated superior tumor targeting effects as compared to free Celastrol control. These results demonstrated that the novel prodrug self-assembled dual-responsive nano-delivery platform was able to improve the bioavailability and tumor targeting activity of Celastrol, which provides a basis for further clinical applications of Celastrol and its derivatives.

Extended author information available on the last page of the article

**Graphical Abstract**

Amphiphilic polymeric prodrug (EDA-GLA/CE/2-FPBA) containing gelatin, lipoic acid, ethylenediamine (EDA), 2-formylphenylboric acid (2-FPBA) was developed, which can self-assembled into micelles in an aqueous solution. Borate ester bond and sulfhydryl groups in the micelles endow the micelles with the ability to respond to high concentration of GSH.

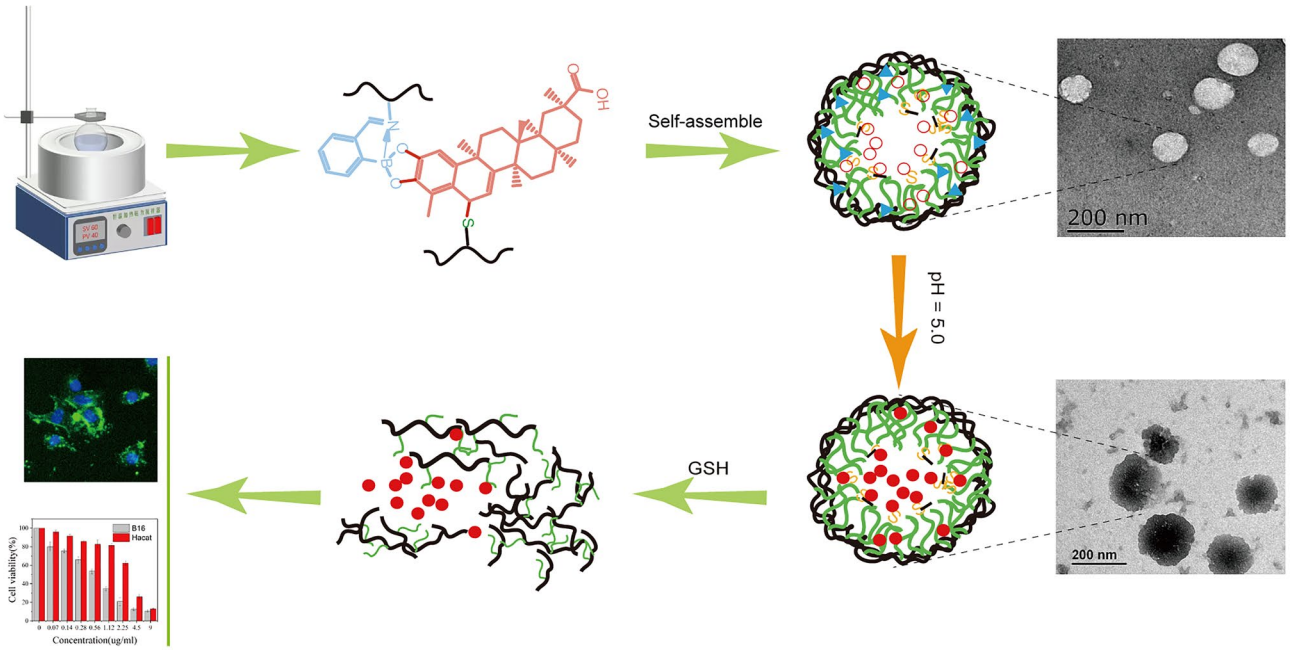


**Keywords** Celastrol · Micelles · Amphiphilic polymer prodrug · Tumor targeting

## 1 Introduction

Cancer is second leading cause of death in the world [1]. Currently, Cancer treatment includes surgery, radiotherapy, chemotherapy and immunotherapy [2–4]. Among all these treatments, Chemotherapy is still the dominant cancer treatment, it can be used as monotherapy or in combination with other therapeutic means [5]. However, chemotherapeutic drugs have many limitations, such as poor water solubility, unspecific killing to normal cells, rapid degradation and clearance in human body, which leads to insufficient concentration of drugs reaching tumor tissues, therefore high concentration drugs or more doses are needed, which cause more severe side effects and reduce drug tolerance of patients [6, 7]. Nanoencapsulation is one of the approaches that may circumvent these restraints. A variety of materials such as polymers, mesoporous silica nanoparticles [8], lipid-based materials, Nanoscale porous organic polymers [9] and Hydrogel [10] could be used as drug delivery platform [11–13]. Among all these materials, amphiphilic polymers are of particular interest due to their unique hydrophobic/hydrophilic structure which can self-assemble into micelles in aqueous environment; Another important fact is that these amphiphilic polymers are constructed using different polymeric blocks. The blocks have numerous functional groups in their molecular chains which can easily be modified to meet the requirement of non-toxic, biocompatible, biodegradable, stability in the systemic circulation and active cancer cell targeting [14, 15]. Chemotherapeutic drugs can be physically entrapped into the micelles core by forming non-covalent bonds such as hydrophobic, hydrogen bond, or ionic interactions. For example, the hydrophobic anticancer drug paclitaxel can be trapped into the core of monomethoxypolyethylene glycol (D, L-lactide) (mPEG-PDLLA) micelles to increase the water solubility of the drug, and reduce the side effects of the drug [16, 17]; The carboxylic acid group of the nonsteroidal anti-inflammatory drug indomethacin can form hydrogen bonds with the amino group of amphiphilic polymer micellar poly (n-isopropylacrylamide) / 4-ethyl aminobenzoate—polyphosphonitrile (PNIPAAm/EAB-PPP), which can form micelles with high drug loading

capacity and achieve sustained release of indomethacin [18]; Wang et al. loaded doxorubicin into gelatin micelles via ion interaction in the mild alkaline environment, and the ion interaction decreases and Doxorubicin is rapidly released from the micelles in the acidic environment of tumor tissue [19]. However, non-covalent bonds loaded drug polymer micelles lack stable dynamic characteristics and are very easy to be affected by complex in vivo environment, leading to premature drug release [20]. Chemical conjugation of drugs to the molecular chain of polymer by covalent bond may solve the problem of premature drug release caused by unstable non-covalent bonds. However, over-stable covalent bond drug loading method may result in insufficient drug liberation from the core at the site of action [21].

Recently, Prodrug-based nanomedicines have attracted the attention of researchers. Unlike physical drug entrapping, in prodrug-based system, parent bioactive drugs were grafted to the main chain or branch chain of polymer via dynamic covalent bonds which response to environmental changes. Under normal physiological conditions, the polymetric prodrug showed strong chemical stability. Some pathological environments such as pH, redox environment, enzymes and hypoxic can trigger the covalent bond break and parent bioactive drug effectively release on action site from the micellar core [22]. Among all chemical bonds, hydrazone, imide and borate bonds are easy to break in acidic environment and disulfide bond is easy to break in high GSH environment, therefore researchers tend to use the above covalent bonds to prepare dynamic covalent polymers. For example, polyethylene glycol (Hydrophilic Terminal) (PEG) covalently combined with doxorubicin (Hydrophobic terminal) through the hydrazone bond to form amphiphilic prodrug polymer PEG-DOX; Capecitabine conjugated with boronic acid-functionalized polycarbonates (PPBC)- polyethylene glycol copolymer (PEGylated-PPBC) via borate bonds to form polymetric prodrug. These prodrugs can self-assembled into micelles and also are pH responsive. They are relatively stable under neutral conditions, and the chemical bond between the drug and polymer breaks in the pathologically weak acidic environment to achieve the dynamic release of the drug [23, 24]. Using ethylene glycol poly(poly(ethylene glycol), researchers covalently combined camptothecin derivative (CPTM) with ethylene glycol Poly (CPTM) using ethylene disulfide bonds to form PEG-b-PCPTM polymer micelles equipped with reductive degradation capabilities. Camptothecin released from micellar under high concentration of glutathione [25]. Therefore, compared with the traditional covalent bond loading mode, the drug release of the dynamic covalent bonded prodrug is triggered by internal and external stimulation, avoiding the premature drug release faced by non-covalent drug loading method.

Celastrol (CE) is a quinone methyl triterpene compound extracted from the root of Tripterygium wilfordii. It has been proven that CE have a variety of biological activities, including anti-oxidation [26], anti-inflammation [27], anti-tumor [28] and anti-angiogenesis [29–34]. However, the low water solubility and high cytotoxicity of CE limit its clinical application. By modifying C-20 and C-3 sites of the A ring to form ester bonds, water solubility of CE was increased, but the biological activity of CE declined either [35]. It has been reported that the nucleophilic part of protein structure can undergo Michael addition with C-6 position of CE structure [36, 37]. Sreeramulu et al. found that under physiological environment, the thiol group of cysteine can undergo reversible Michael addition reaction with C-6 site of CE structure [38], and when the pH decreases, the reaction goes in the opposite direction to produce free CE. This property could be used as the theoretical basis for designing CE polymer prodrug.

Here, we report the design, synthesis, and characterization of a dual-responsive amphiphilic CE-polymer prodrug based on gelatin, lipoic acid, ethylenediamine (EDA), 2-formylphenylboric acid (2-FPBA) and CE. First, we prepared EDA-gelatin-lipoic acid derivative (EDA-GLA) via stepwise synthesis, then the derivative was conjugated to the C-6 position of CE by Michael addition of sulfhydryl group, forming CE-EDA-GLA. 2-formylbenzoylboric acid (2-FPBA) crosslinked with EDA-GLA derivative and CE-EDA-GLA via imide bond, borate ester bond. The polymer can self-assembled into micelles with a hydrophobic CE core and hydrophilic EDA-GLA shell in aqueous solution. In addition, the excess sulfhydryl groups in the micelles crosslinked with each other to form disulfide bond which could not only maintain stability of the micelles, but also endow the micelles with the ability to respond to high concentration of GSH. Next, we investigated the pH and GSH responses of prodrug micelles and drug release behavior. The cytotoxicity of free CE and CE-prodrug polymer micelle to normal and melanoma cells and the uptake of CE-prodrug polymer micelles by melanoma cells were then compared. Our work is expected to provide a novel approach to prepare tumor-targeting CE prodrug micelles to improve the clinic translation potential of CE.

## 2 Materials and methods

### 2.1 Materials

Gelatin type B (MW: 50,000–100000), lipoic acid (LA), 1-ethyl -(3-dimethylaminopropyl) carbamyldiimide (EDC), n-hydroxysuccinimide (NHS), ethylenediamine (EDA), 2-formylphenylboric acid (2-FPBA), triwiline (Celastrol), Tri (2-carboxylethyl) phosphine (TCEP), fluorescein

isothiocyanate (FITC) were obtained from Sino Pharm. All chemicals and reagents used in the study were of analytical grade or higher.

## 2.2 Methods

### 2.2.1 Preparation of the EDA-GLA derivative

**2.2.1.1 Synthesis of GLA** 260 mg lipoic acid (LA) was suspended to 20 ml 60% ethanol, and 1 M sodium hydroxide solution was used to adjust pH to 5.9–6.0. 310 mg EDC and 200 mg NHS were added to the suspension with stirring at 37℃ for 25 min to activate LA. 250 mg B gelatin was dissolved into 30 ml of 60% ethanol, and stirred at 50℃ until the solution turned clear, then poured in the activated LA solution. The reaction mixture was stirred at 37℃ for 16 h. At the end of the reaction, ethanol was added to precipitate the resulting GLA. After centrifugation (5000 rpm) for 20 min, GLA was collected and rinse three times with anhydrous ethanol and a small amount of distilled water was used to remove residual ethanol, unreacted lipoic acid and gelatin. GLA was redissolved in 10 ml of water, and the solution was lyophilized for 48 h to obtain a white fluffy powder, which was stored in vacuum for later use, the yield of GLA was about 56%.

**2.2.1.2 Synthesis of EDA-GLA** 500 mg GLA was dissolved in 30 mL of deionized water, 1.5 mL ethylenediamine was added into GLA solution, After the pH was adjusted to pH5 with concentrated hydrochloric acid, 0.9 g EDC was added to above mixture with stirring at 37 °C for 24 h. The resulting reaction solution was put into a dialysis bag (MWCO 3500) for dialysis in distilled water for 48 h, and the dialysate was lyophilized for 48 h. The resulting white fluffy powder was stored in a vacuum for later use, the yield of EDA-GLA was 68%.

### 2.2.2 Preparation of the EDA-GLA/CE/2-FPBA micelles

**2.2.2.1 Ring-opening of GLA in EDA-GLA** 300 mg EDA-GLA was dissolved in 60 mL of 0.01 M PBS (pH 5.0), and stirred until completely dissolved at room temperature. 100 mg TCEP was added and protected with nitrogen at room temperature for 16 h. The resulting Re-EDA-GLA solution was put into dialysis bag (MWCO 3500) and dialysis in distilled water (pH4.0) for 48 h. After the dialysate was freeze-dried for 48 h, the white fluffy powder was obtained and stored in vacuum for later use, the yield of this reaction was 90%.

**2.2.2.2 Synthesis of EDA-GLA/CE/2-FPBA** 40 mg of Re-EDA-GLA dissolved in 40 mLof 0.01 M PBS (pH5.0) with stirring at room temperature. 4 mg CE in 4 ml of DMSO then added into above solution, the pH value was adjusted to 7.4 with 1 M sodium hydroxide solution. 3.9 mg of 2-FPBA was added and stirred at 8℃ for 12 h. The reaction solution was put into a dialysis bag (MWCO 3500) and dialyzed in distilled water at 8℃ for 24 h. After lyophilization of dialysate for 48 h, white fluffy powder was collected and stored in vacuum for reserve, the yield of this reaction was 53%.

### 2.2.3 Micellar characterization

**2.2.3.1 Particle size and zeta potential** A dynamic light scattering analyzing (DLS) was conducted to measure the size and ζ potential of GLA/CE/2-FPBA micelle using the Zetasizer (Nano ZS, Malvern Co., UK). Briefly, 1 mg/ml of EDA-GLA/CE/2-FPBA in 0.01 M PBS (pH7.4) was prepared. 1 ml of sample solution was used.

**2.2.3.2 Transmission electron microscopy (TEM)** The morphology of EDA-GLA/CE/2-FPBA micelles was observed by transmission electron microscopy (TEM) (JEM-1230HC, Tokyo, Japan). Briefly, 1 mg/ml EDA-GLA/CE/2-FPBA was prepared with 0.01 M PBS (pH7.4) buffer and then dropped onto a carbon-coated copper grid, stained with 2% (w/v) phosphotungstic acid for 2 min, dried before observation.

### 2.2.4 The release of CE from micelles in vitro

The release of EDA-GLA/CE/2-FPBA in vitro was studied by dialysis method. 10 mg of EGEF was dissolved in 4 ml of PBS (7.4), 4 ml of PBS (5.0); 4 ml of PBS (7.4) containing 10 mM GSH and 4 ml of PBS (5.0) containing 10 mM GSH. The above four groups of sample solutions were put into 4 dialysis bags (MWCO 3500), and soaked in 60 ml of the corresponding release medium, and incubated in 37 °C constant temperature shaker, at 1 h, 6 h, 12 h, 24 h, 48 h, 72 h, 96 h, 120 h, 144 h and 168 h, 2 ml of sample solution was collected and 2 ml of corresponding fresh release medium was added. The concentration of released tripterine was measured by a UV–Vis spectrophotometer, and the percentage of released drug was plotted against time.

### 2.2.5 In vitro anticancer activities

Melanoma cellB16F10) and normal epithelial cells (HaCat) were seeded into 96-well plates at a density of $1 \times 104$ cells per well and incubated in RPMI 1640 medium and MEM medium containing 10% FBS and 1% PS respectively in an incubator with 5% CO2 at 37 °C. After 24 h, cells were treated with different concentration of EDA-GLA/CE/2-FPBA (0,0.39, 0.78125, 1.5625, 3.125, 6.25, 12.5, 25and 50 μg/mL. After 24 h incubation, 40 μl of 3- (4,5)

-dimethylthiazolide (-Z-Y1) -3, 5-dibenzothiazolide (MTT) was added to each well and cultured at 37 °C and 5%CO2 for 4 h. After the incubation, the MTT was removed from each well and 150 µl DMSO was added to dissolve the formazan crystals. The absorbance was recorded at 490 nm using a microplate reader. The experiments were performed in triplicates, and cells without any treatment were used as the control [39, 40].

Cell viability (%) =As/Ac×100%

As is the light absorption value of cell sample, and Ac is the control light absorption value.

#### 2.2.6 Cellular uptake of EDA-GLA/CE/2-FPBA micelles

B16F10 were seeded into 24-well plates at a density of 1 × 105 cells per well. 1 ml of RPMI-1640 medium containing 10% fetal bovine serum and 1% penicillin plus streptomycin were added to each well and cultured at 37 °C and 5%CO2. After 24 h incubation, the medium was replaced with fresh PMI-1640 medium solution containing FITC-labeled EGEF micelles (the concentration of FITC-labeled EDA-GLA/CE/2-FPBA micelles was 300 µg/ml) and cultured at 37 °C and 5%CO2. After incubation for 4 h, the medium in each well was removed and the cells were washed with PBS for at least three times, and fixed with 4% paraformaldehyde, and then cells were stained with DAPI solution. The prepared covered slips were observed with a living cell imager.

#### 2.2.7 Statistical analysis

All data were expressed as mean ± standard deviation (SD), and the differences between experimental groups and control group were compared using Student's t-test. Statistical significance was established at $P < 0.05$.

## 3 Results and discussion

### 3.1 Synthesis and characterization of EDA-GLA/CE/2-FPBA prodrug polymer

In drug delivery, the building blocks of polymers have a great influence on the drug loading efficiency, drug release kinetics and drug biocompatibility. Therefore, in this study, we choose gelatin and lipoic acid as main blocks of polymer, as both of them has been used for biomedical purpose [41, 43]. First, we synthesized the EDA-GLA polymer skeleton. As shown in Fig. 1, Gelatin (G) and lipoic acid (LA) formed lipoic acid gelatin (GLA) via EDC/NHS coupling chemistry. The synthesis of lipoic acid Gelatin (GLA) was controlled by adjusting the feed ratio of Gelatin to lipoic acid, reaction temperature and reaction time. Our results showed that the feed ratio of gelatin to LA at 1:1 and the reaction

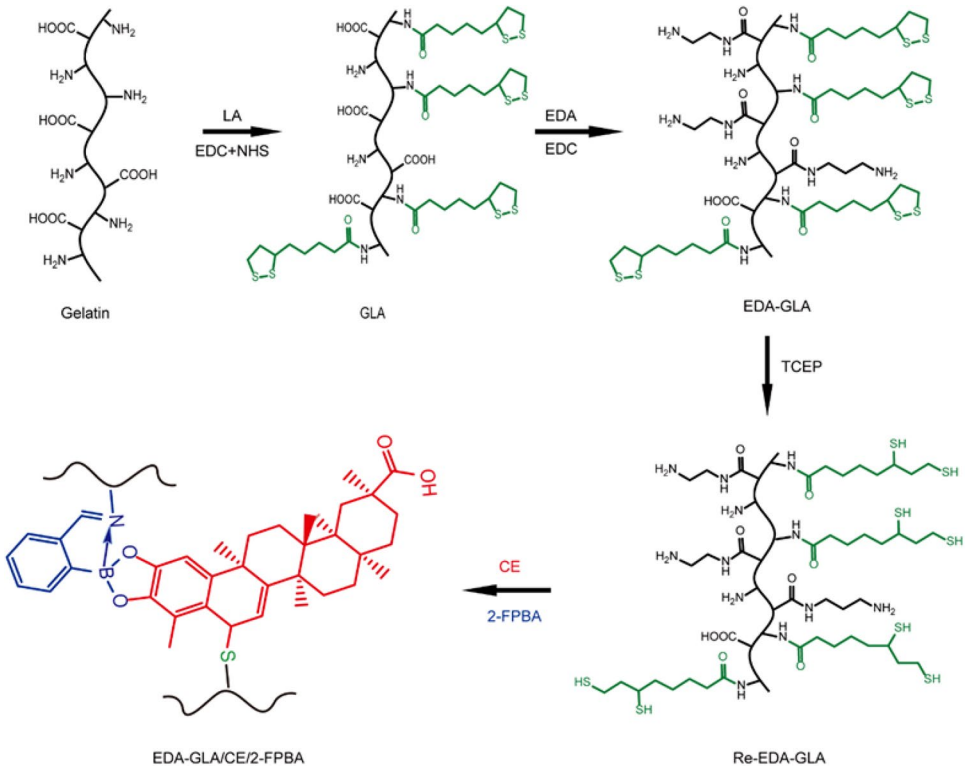


**Fig. 1** The Synthesis route of the designed EDA-GLA/CE/2-FPBA prodrug polymer

temperature was set to be 37 °C resulted in the maximum degree of substitution (DS) of Gelatin. To incorporate CE, 2-FPBA to GLA main chain, ethylenediamine (EDA) was first reacted with GLA to form EDA-GlA to obtain free amino groups, then the five-membered heterocyclic ring of lipoic acid residue on EDA-GLA was opened with strong reducing agent TCEP to produce sulfhydryl groups (Re-EDA-GLA). Finally, amphiphilic EDA-GLA/CE/2-FPBA prodrug polymers were prepared by one-pot method. In the preparation process, the sulfhydryl groups of Re-EDA-GLA first reacted with C-6 site of CE to form EDA-GLA-CE under physiological conditions (pH 7.4). Using 2-FPBA as a linker, the free amino group of Re-EDA-GLA and C-6 site of CE were subjected to the Michael addition reaction to form a catechole-coupled polymer, which could self-assemble into micelle with a hydrophilic shell formed by gelatin derivatives and a hydrophobic core formed by CE.

The structure of EDA-GLA/CE/2-FPBA was first confirmed by 1H NMR (Fig. 2A). A group of new proton peaks appeared in the range of 5.5 ppm ~ 8.5 ppm, wherein peak A: 8.35 ppm was assigned to – N = CH2—of proton peak, which suggested that benzoic imine conjugate structure

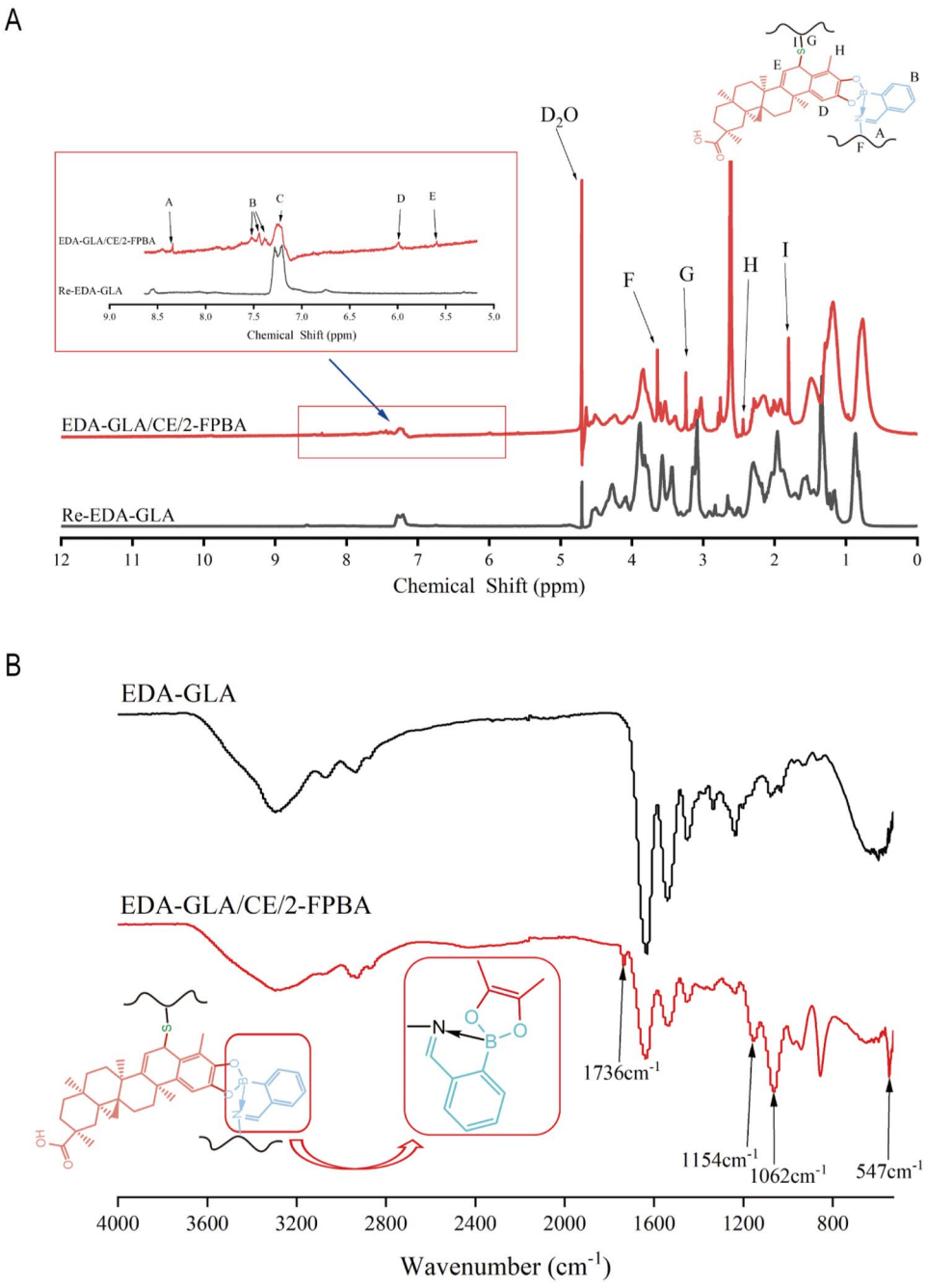


**Fig. 2** Chemical structure characterization of EDA-GLA/CE/ 2-FPBA. **A** 1H NMR NMR spectra of Re-EDA-GLA and EDA-GLA/CE/2-FPBA. **B** Infrared spectra of Re-EDA-GLA and EDA-GLA/CE/2-FPBA

was formed. Peak B: 7.39 ppm, 7.44 ppm and 7.54 ppm are the characteristic peaks of aromatic hydrogen of 2-FPBA benzene ring; These results demonstrated successful combination between gelatin and 2-FPBA. Peak C is the unique peak of gelatin. Peak D: 6.00 ppm is the characteristic peak of aromatic hydrogen on the A ring of CE structure. Peak E: 5.60 ppm is the olefin hydrogen peak of C-7 in the CE structure. The FT-IR is utilized to examine the chemical structure [43–45]. The FT-IR spectrum of EDA-GLA/CE/2-FPBA prodrug polymer (Fig. 2B) showed, compared with EDA-GLA, EDA-GLA/CE/2-FPBA showed characteristic peaks at 1736 $cm^{-1}$, 1154 $cm^{-1}$, 1062 $cm^{-1}$, 547 $cm^{-1}$, etc. Among them, 1736 $cm^{-1}$ belongs to the C = N bond, indicating that the carbonyl group in 2-FPBA combines with the amino group on the main chain of EDA-GLA to form a Schiff base. It has been reported that the infrared absorption peaks of C-O stretching vibration, B-O stretching vibration and out-of-plane vibration of borate are around 1220 $cm^{-1}$, 1000–1090 $cm^{-1}$ and 500–750 $cm^{-1}$, respectively, in phenyl borate fat bond [46]. Consistent with the results reported in above scientific paper, characteristic peak at around 1154 $cm^{-1}$ appeared in the FT-IR spectrum of EDA-GLA/CE/2-FPBA prodrug polymer, which may be attributed to C-O stretching vibration, peak at 1062 $cm^{-1}$ may attributed to B-O stretching vibration, and peak at 547 $cm^{-1}$ may attributed to out-of-plane vibration of borate. These results also demonstrated that CE was successfully bound to the mercaptogroup of the lipoic acid residues in EDA-GLA and formed a borate bond with 2-FPBA and further confirmed that 2-FPBA and CE had been successfully grafted onto the main chain of EDA-GLA.

In the ultraviolet map (Fig. 3A), CE in DMSO solution presented its unique absorption peak(425 nm), while EDA-GLA/CE/2-FPBA micelles did not, indicating that CE has been grafted to EDA-GLA polymer and its long-conjugated structure has been destroyed and its orange color has disappeared, which is consistent with literature reports [38]. However, the absorption peak of EDA-GLA/CE/2-FPBA micelle appeared at 450 nm after acid destruction, indicating that CE had been removed from the main chain of EDA-GLA polymerization and the long-conjugated structure reformed. Due to the influence of solvent and micellar solubilization, the absorption peak was red shifted from 425 to 450 nm. DSC is used to study the thermal properties of the polymers [47]. The DSC curves (Fig. 3B) showed that compared with the EDA-GLA polymer, the mixture of EDA-GLA and CE had an obvious exothermic peak at 226℃, indicating that no covalent bond was formed between CE and EDA-GLA, and CE was volatilized. However, the EDA-GLA/CE/2-FPBA micellar has no exothermal peak at 226 °C, and the baseline of the entire curve is relatively stable, which is significantly different from the curve of EDA-GLA polymer, indicating that CE and EDA-GLA have formed covalent bonds to form new substances, which also proved that CE has been successfully grafted onto the side chain of EDA-GLA.

In addition, since C-6 of CE forms catechol structure after Michael addition reaction and its stability is extremely poor, characteristic peak from catechol structure appeared in neither infrared and nor nuclear magnetic spectrum. Therefore, we refer to the method reported in literature [48]. Phenylboric acid in the structure of 2-(4-dihydroxyborane) phenyl-4-carboxyquinoline (Fluorescent Ingredient) was used, which can form borate bond with the structure of catechol. Photoinduced electron transfer effect transferred the electrons of catechol to quinoline and changed the fluorescence intensity of 2-(4-dihydroxyborane) phenyl-4-carboxyquinoline(FI), which could indirectly prove the formation of catechol structure. As shown in the Fig. 4A, the emission wavelength of 2-(4-dihydroxyborane) phenyl-4-carboxyquinoline was redshifted from 392.2 nm to 397.9 nm in the EDA-GLA polymer solution, and the fluorescence intensity increased from 16,679 to 17,432. When CE were added into above EDA-GLA polymer solution, the fluorescence intensity of 2-(4-dihydroxyborane) phenyl-4-carboxyquinoline decreased further, and the increasing of CE concentration showed a negative relationship with

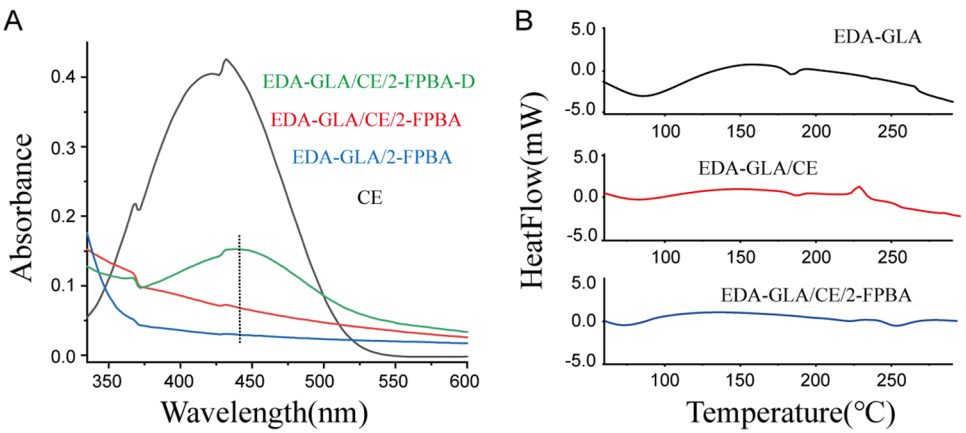


**Fig. 3** **A** UV absorption maps of CE, EDA-GLA/2-FPBA, EDA-GLA/CE/2-FPBA and EDA-GLA/CE/ 2-FPBA-D(Acid Destruction). **B** Differential scanning calorigrams of EDA-GLA, EDA-GLA@CE and EDA-GLA/CE/2-FPBA

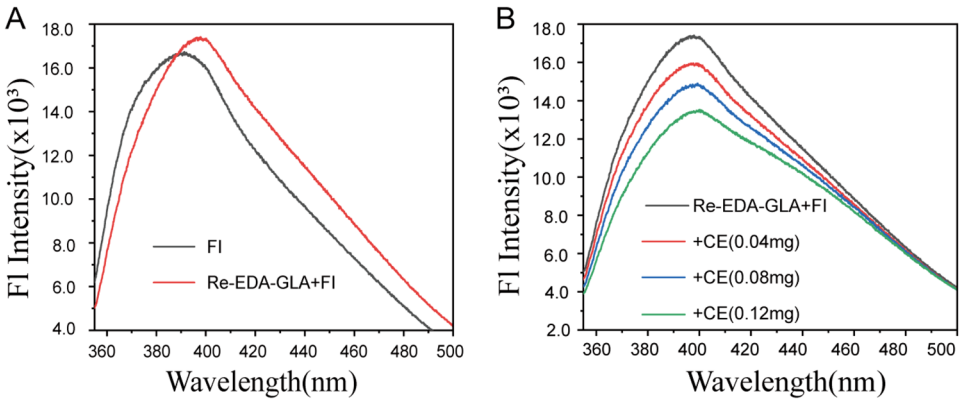


**Fig. 4** **A** Fluorescence intensity diagram of Re-EDA-GLA and FI(2-(4-dihydroxyborane) phenyl-4-carboxyquinoline), excitation wavelength is 337 nm. **B** Diagram of the influence of different concentrations of CE on the fluorescence intensity of FI, and the excitation wavelength is 337 nm

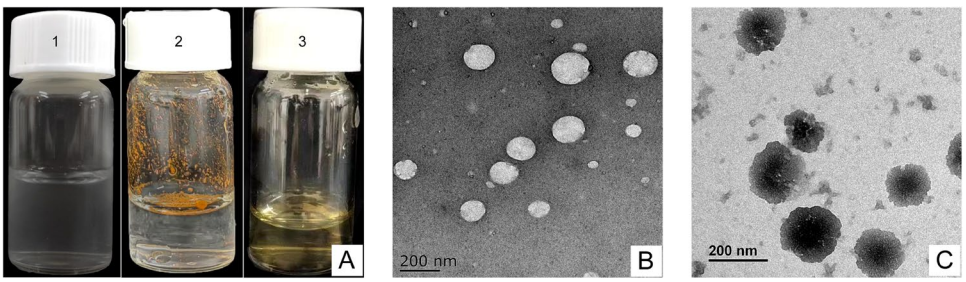


**Fig. 5** **A** Appearance of EDA-GLA/CE/2-FPBA micelles (pH 7.4)(bottle1), free CE in aqueous solution(bottle2), EDA-GLA/CE/2-FPBA micelles (pH 5.0) (bottle3). **B** TEM images of EDA-GLA/CE/2-FPBA micelles under pH 7.4. **C** TEM images of EDA-GLA/CE/2-FPBA micelles under pH 5.0

**Table 1** Particle size, PDI and Zeta potential of EDA-GLA/CE/2-FPBA micelles

| Dispersion medium | Size (nm) | PDI | Zeta |
|---|---|---|---|
| 0.01 M PBS (pH 7.4) | 292.27 ± 13.52 | 0.268 ± 0.041 | 5.37 ± 0.35 |
| DMSO (1:10 m:V) | 709.00 ± 426.11 | 0.481 ± 0.371 | – |

CE concentration (Fig. 4B), which indirectly proved that CE was grafted onto gelatin molecules and formed the structure of catechol. Taken together, all these results demonstrated EDA-GLA/CE/2-FPBA prodrug polymer successfully synthesized.

## 3.2 Self-assembly and characterization of EDA-GLA/CE/2-FPBA prodrug micelles

Due to the present of hydrophilic parts of EDA-GLA and hydrophobic parts of CE, EDA-GLA/CE/2-FPBA prodrug polymers can self-assembled into micelle in aqueous solution. The self-assembled micelles can completely dissolve in aqueous solution, Colorless EDA-GLA/CE/2-FPBA micellar solution confirmed that C-6 position of CE is grafted onto the EDA-GLA polymer, because when the C-6 position of CE is occupied, the long-conjugated structure is destroyed and the red brown color disappears (Fig. 5A bottle1); free CE negligibly dissolved (Fig. 5A bottle2). The self-assembled CE prodrug micelles were spheres (Fig. 5B) with diameters of about 292.27 nm in 0.01 M PBS (pH 7.4) buffer, and the PDI was about 0.268 in aqueous solution (Table 1). When EDA-GLA/CE/2-FPBA micelles were incubated with PBS (pH5.0) buffer for 96 h, the EDA-GLA/CE/2-FPBA micellar solution changed from colorless to clear yellow solution, indicating that CE has been shed from the EDA-GLA polymer, but CE is still in the micelle, as no CE precipitation appeared in the solution (Fig. 5A Bottle 3). In addition, TEM image showed that the shape of EDA-GLA/CE/2-FPBA micelles changed to irregular spherical shape, after 96 h incubation with PBS (pH5.0) buffer (Fig. 5C), as when new chemical bond break or form, the morphology of the nanoparticle changed [49, 50]. These results agreed with our anticipation that the phenylborate ester bond between 2-FPBA and CE could degrade in tumor cell microenvironment (pH 5.0), resulting in CE shedding from the main chain of EDA-GLA. However, the main spherical shape skeleton was not destroyed, because the sulfhydryl group in EDA-GLA can form disulfide bonds to cross-link the micellar shell, improving stability of the micelles. When EDA-GLA/CE/2-FPBA micelles dissolved in DMSO organic solution with a mass volume ratio of 1:10, the particle size of micelles increased from 292.27 nm to 709.00 nm, and PDI increased to 0.481, but its particle size signal did not disappear like non-crosslinked micelles (Table 1). This further confirmed the shedding of CE, and the integrity of the EDA-GLA shell.

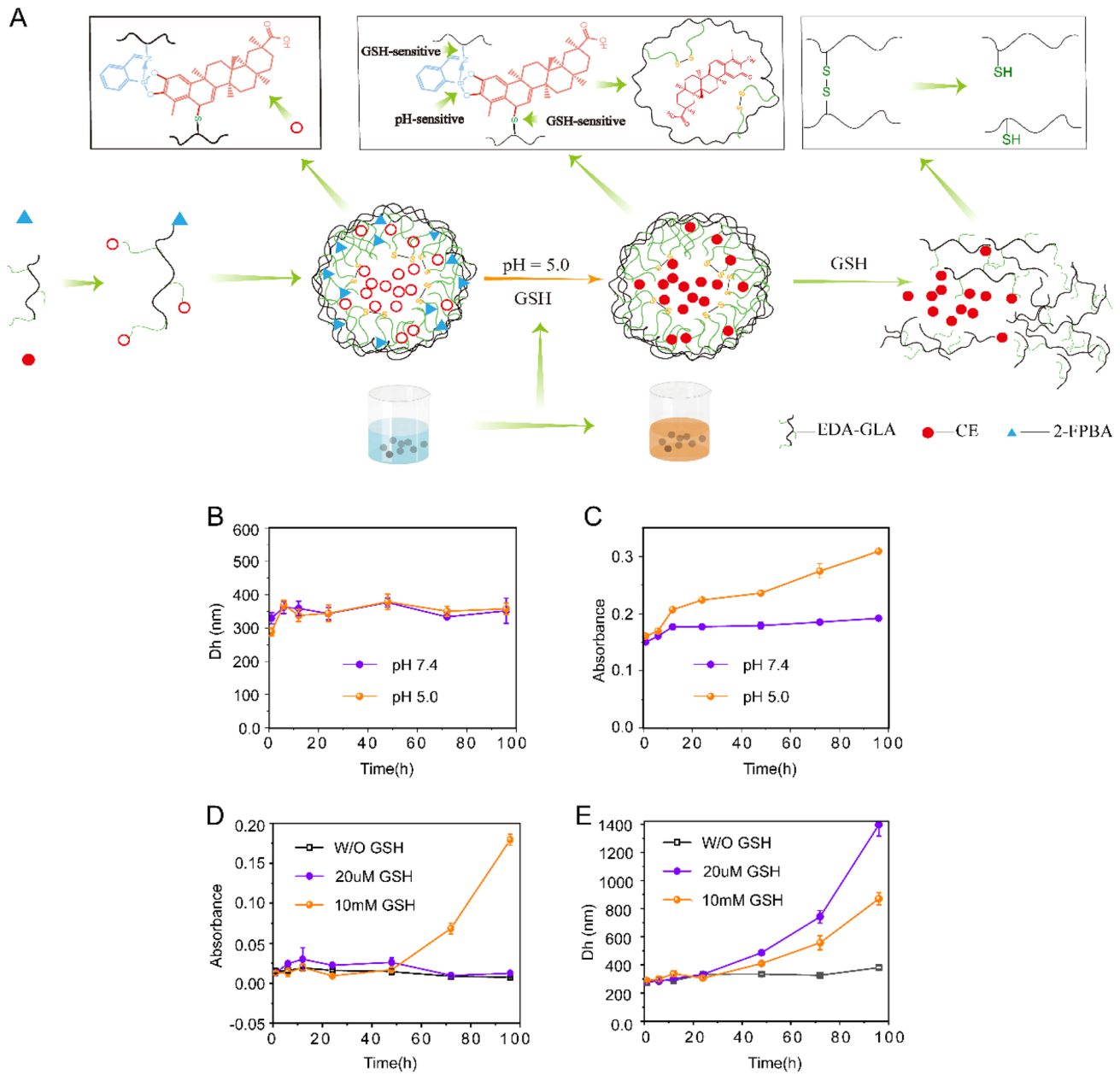


**Fig. 6** **A** Schematic Illustration of EDA-GLA/CE/2-FPBA micellar self-assembly and dual response drug release. **B** The particle size of EDA-GLA/CE/2-FPBA micelles in PBS 7.4 and PBS 5.0 at different testing time points. **C** Absorbance of EDA-GLA/CE/2-FPBA micelles at 450 nm in PBS 7.4 and PBS 5.0 within the tested periods. **D** Absorbance of EDA-GLA/CE/2-FPBA micelles at 450 nm in PBS 7.4 in the present or absent of GSH. **E** The particle size of EDA-GLA/CE/2-FPBA micelles in PBS 7.4 in the present or absent of GSH

### 3.3 In vitro pH and GSH response drug release

In the EDA-GLA/CE/2-FPBA prodrug polymer, one end of the CE (Red molecule in Fig. 6A) was conjugated to 2-FPBA (blue molecule in Fig. 6A) on the main chain of EDA-GLA/2-FPBA through borate ester bonds. The other end of the CE covalently bonded with EDA-GLA part of the EDA-GLA/ 2-FPBA through thioether bond. Formed EDA-GLA/CE/2-FPBA amphiphilic molecule has EDA-GLA as a hydrophilic end and CE/2-FPBA as a hydrophobic end. Once the prodrug polymer self-assembled into micelles, the excess sulfhydryl groups of EDA-GLA form disulfide bonds, enhancing the stability of the micelles. The borate ester bonds are stable under physiological conditions (pH7.4), but can be degraded under weak acidic conditions (such as pH 5.0 in the endosome of tumor cells) [24, 51–53]. Once borate

bond broken, CE is shed from the main chain of the polymer (Fig. 6A), But still trapped inside the core of micelles, high concentration of GSH can break down the thioether bond and disulfide bonds, eventually free CE released.

To verify the pH responsiveness of EDA-GLA/CE/2-FPBA pro-drug micelles, changes in the particle size of micelles in PBS under different pH values and the absorbance of micellar solution at 450 nm (CE solution has strong absorption at 450 nm) were monitored over 96 h. No obvious change in particle size was observed at pH 7.4 and pH 5.0(Fig. 6B). In contrast, a gradually increase was observed during the testing time in the absorption value of CE prodrug micelles solution at 450 nm when they were incubated in PBS at pH 5.0, which is contributed to free CE(Fig. 6C). This indicated that CE was gradually dissociated from the main chain of the polymer due to the fracture of borate ester bond, which resulted in the increasing release of CE with the increase of time. These results were consistent with our hypothesis that the EDA-GLA/CE/2-FPBA pro-drug micelles are pH responsive, but free CE is still trapped inside the micelles shell, as shown in Fig. 6A.

It has been reported that the concentration of glutathione (GSH) in tumor cells is over 1000-fold higher than in blood and much higher than that in normal cells [54, 55]. The disulfide bond can be reduced to the hydrophilic thiol group by GSH. Therefore, the disulfide bond has been widely used to design GSH-responsive drug delivery system, which could facilitate specifically release of parent drugs [56, 57]. In the EDA-GLA/CE/2-FPBA prodrug polymer, the sulfhydryl group produced after the lipoic acid residues on EDA-GLA were reduced by TCEP. CE was reacted with sulfhydryl group by Michael addition reaction. When the EDA-GLA/CE/2-FPBA prodrug polymer self-assembled in aqueous solution, the excess sulfhydryl groups are self-crosslink to form disulfide bonds within the shell of the micelles, which can be destroyed by high concentrations of GSH in cancer cells, leading to drug release, which is the theoretical basis for our initial design of GSH responsive micelles (Fig. 6A). To investigate the responsiveness of the prodrug micelles to GSH, we examined the absorbance of released CE at 450 nm and changes in the particle size of micelles in PBS (pH 7.4) in the present or absent of GSH. As shown in the Fig. 6D, under pH 7.4 in the absent of GSH, the absorbance and particle size of the micelle's solution have no significant changes. When GLA/CE/2-FPBA prodrug micelles incubated with 20 μM GSH (GSH concentration in normal cells), absorbance of CE at 450 nm did not increase (Fig. 6D), but a greater increase in the size of GLA/CE/2-FPBA prodrug micelles was detected within the tested time (Fig. 6E) which contributed to the cleavage of GSH-sensitive disulfide bonds within the micellar shell. When the concentration of GSH reached to 10 mM (GSH concentration in tumor cells), the absorbance at 450 nm increased dramatically after 50 h incubation, however particle size gradually increased with time, compared with 20uM GSH treatment, the size of micelles decreased instead, which indicated that under high concentration of GSH, the micelles have started dissembled completely. Taken together, GLA/CE/2-FPBA prodrug micelles demonstrated GSH and pH responsiveness, which could be beneficial to the controlled release of chemical drugs.

### 3.4 Release of CE in vitro

After investigating the drug release of GLA/CE/2-FPBA prodrug micelles, we investigate the CE release profiles in vitro at pH7.4 and pH5.0. The cumulative release of the CE was measured by monitoring the UV absorption value of free CE in the dialysate at 425 nm. As shown in Fig. 7, after incubation for 7 days, less than 3% of CE was slowly released from the micelles at pH 7.4 and pH 5.0, no significant differences observed between two groups, indicating that although under low pH, CE in micelles fell off the backbone of the EDA-GLA polymer due to the cleavage of the borate bond and C-S bond which cross-link CE to the backbone of the polymer, the micellar shell is still keeping integrity by disulfide bonds, and free CE is still locked in the nucleus of the micelles. This also explains the phenomenon in Fig. 5A that the EDA-GLA/CE/2-FPBA micellar solution changed from colorless to clear yellow solution under pH 5.0, but no CE precipitation appeared in the solution, because CE is still locked in the micelle shell. When 10 mM GSH was added, the cumulative release of CE from the micelles was significantly

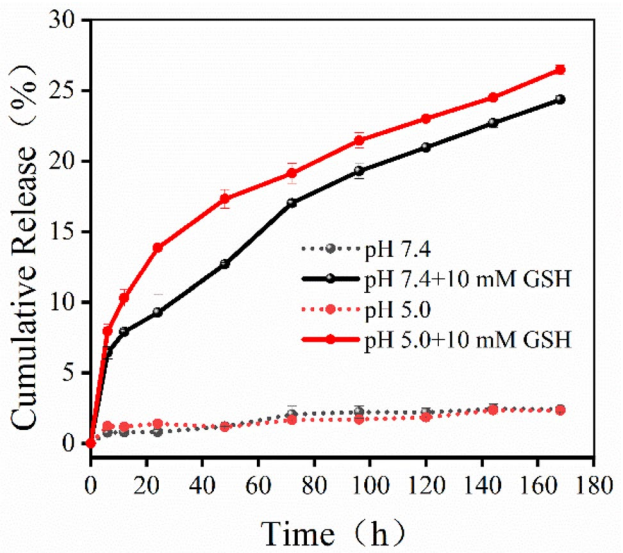


**Fig. 7** In vitro release of CE from EDA-GLA/CE/2-FPBA prodrug micelles at different pH values in the present or absent of GSH (mean ± SD, $n = 3$)

increased to 24.3.15% at pH 7.4 and 26.5% at pH 5.0 owing to rupture of disulfide bonds linkage triggered by GSH and micelle shell dissociated gradually, which was in accordance with the particle size changes of micelles triggered by GSH in Fig. 6E. All these results indicated that EDA-GLA/CE/2-FPBA micelles were responsive to both pH and GSH,

### 3.5 Cytotoxicity and cellular uptake of EDA-GLA/CE/2-FPBA micelles in vitro

Furthermore, we used MTT method to evaluate the growth inhibition effects of free CE, EDA-GLA/CE/2-FPBA micelles and EDA-GLA/2-FPBA against normal cell line HaCat and melanoma cell line B16. As shown in Fig. 8A, the blank polymer carrier EDA-GLA/2-FPBA showed no significant cytotoxicity after co-culture with B16 and HaCat

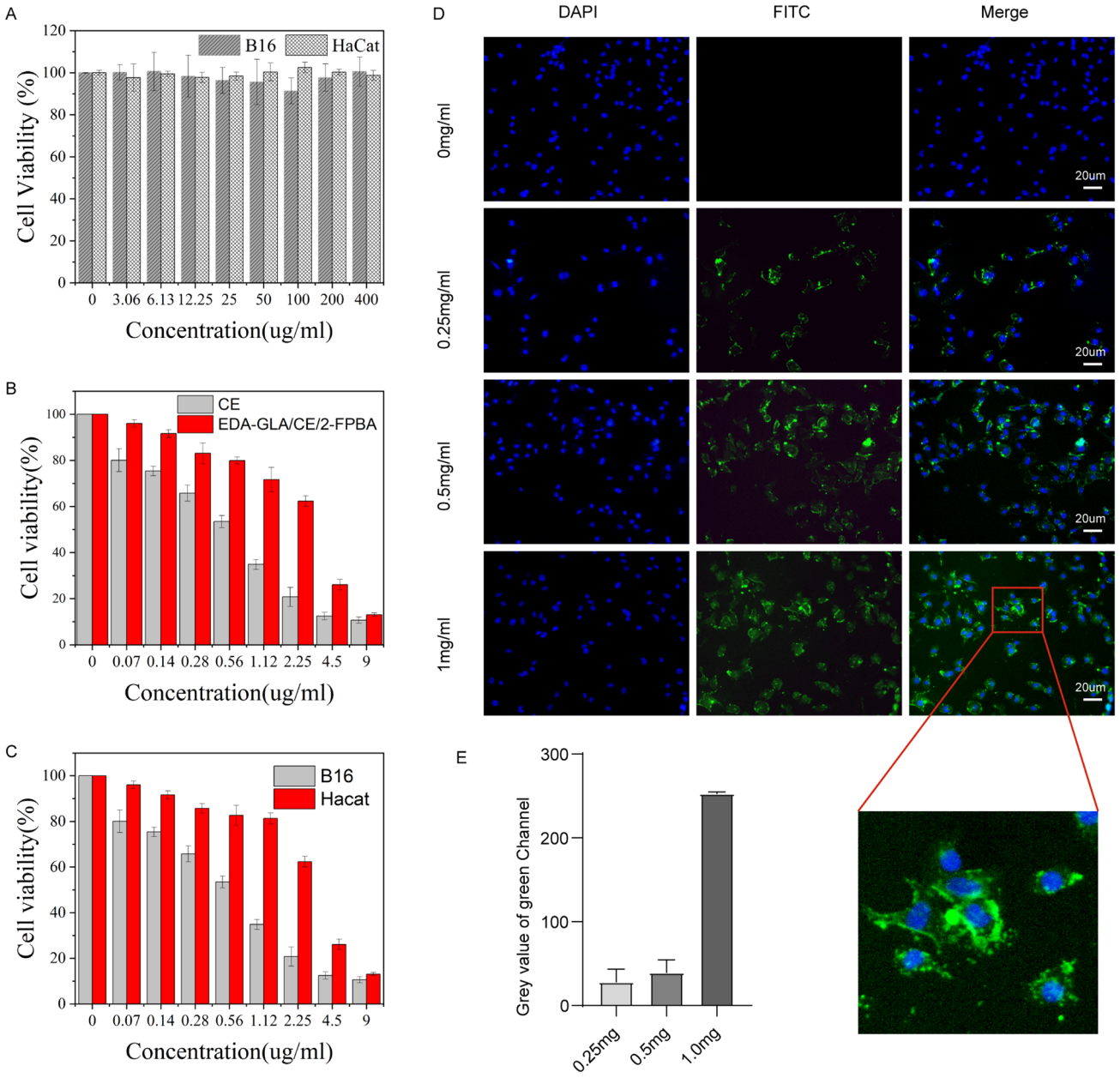


**Fig. 8** In vitro cytotoxicity and cell uptake of micelles. **A** EDA-GLA/2-FPBA drug carrier against HaCat and B16 (mean ± SD, $n = 5$), **B** free CE, EDA-GLA/CE/2-FPBA micelles against B16, **C** EDA-GLA/CE/2-FPBA micelles against B16 and HaCat, **D** Fluorescence microscopy images of B16 after incubation with FITC- EDA-GLA/2-FPBA for 4 h. Blue and green represent DAPI and FITC, respectively. **E** Fluorescence intensity in 100 cells was measured by image pro plus 6.0 and plotted

cells for 48 h, indicating that the safety of polymer carrier EDA-GLA/2-FPBA as a drug carrier. The cell growth inhibition of free CE and EDA-GLA/CE/2-FPBA micelles against B16 cells and HaCat cells was also evaluated. As shown in Fig. 8B, both free CE and EDA-GLA/CE/2-FPBA showed dose-dependent antitumor activities against B16 after 48 h treatment. Free CE exhibited greater inhibition effects than EDA-GLA/CE/2-FPBA micelles owing to the low pH and high GSH triggered controlled drug release. In contrast, EDA-GLA/CE/2-FPBA micelles showed high cell viability against HaCat cells in relative to free CE (Fig. 8C). This indicated that the EDA-GLA/CE/2-FPBA micelles are more likely to release CE in tumor cells and the toxicity of EDA-GLA/CE/2-FPBA micelles to normal cells is significantly reduced. The reason is that the weak acid (pH 5.0) environment and high GSH (10 mM) concentration in tumor cells promote CE release.

To study the cellular uptake of EDA-GLA/CE/2-FPBA micelles, EDA-GLA/CE/2-FPBA micelles were labeled with FITC. As shown in Fig. 8D, different concentration of the FITC-EDA-GLA/CE/2-FPBA micelles were co-cultured with B 16 cells for 4 h, and the green fluorescence was primarily appeared in the cytoplasm of B16 cells, and showed dose-dependent fluorescence intensity (Fig. 8E), indicating that the EDA-GLA/CE/2-FPBA micelles could be effectively uptake by B16 cells.

## 4 Conclusion

pH- responsive drug loading and releasing nano drug system draw a lot of attention these years, as tumor tissue has acidic environments compared with normal tissue, each systems exhibited their own stimulative mechanism based on chemical structures such as Yanet et al. prepared a biblock copolymer (PEG-B-PPBC), antitumor drug capecitabine (CAPE) is grafted onto the hydrophobic end side chain of PEG-b-PPBC by borate bond to form a polymer prodrug. CAPE can be released under weak acid environments (pH 6.5 or pH 5.5) due to borate ester bond are stable under physiological conditions (pH 7.4), degraded in the weak acid environment [24]; Qin et al. synthesized tumor-targeted ultra-pH-responsive conjugates PBA/Dex-gOE, dextran acted as a stabilizing and surface-modifying agent. The PBA/Dex-g-OE micelles possessed high stability in physiological condition and were pH sensitive to both extracellular and intracellular acidic conditions [58].

In this study, we designed and developed an EDA-GLA/CE/2-FPBA polymer prodrug via the conjugation of the gelatin derivatives EDA-GLA, 2-FPBA and quinone methyl triterpene CE under physiological conditions (pH 7.4) through dynamic reversible covalent bond. The amphiphilic EDA-GLA/CE/2-FPBA polymer prodrug could be self-assembled into micelles. The micelles are stable under physiological conditions, borate ester bond cleavage happened under weak acid condition, bioactive CE was produced, but still trapped inside the core of micelles, as the shell of micelles is still not disrupted yet owing to the disulfide bonds within micelles. High GSH conditions destroyed disulfide bond, eventually CE released. The micelles exhibit high cellular uptake in tumors B16 cells. EDA-GLA/2-FPBA drug carrier had negligible toxicity to cells. Furthermore, EDA-GLA/CE/2-FPBA micelles displayed higher cell inhibition ability to tumor B16 cells than to normal HaCat cells. These results suggested that EDA-GLA/CE/2-FPBA polymetric prodrug is a stable, intelligent and safe antitumor delivery system for cancer chemotherapy.

**Acknowledgements** This research was funded by the Collaborative Grant-in-Aid of the HBUT National "111" Center for Cellular Regulation and Molecular Pharmaceutics (XBTK-2021009) and Research Funds from Hubei University of Technology(GCRC20200013).

## Declarations

**Conflict of interests** The authors declare that there is no conflict of interests, we do not have any possible conflicts of interest.

## References

1. X. Wang, L. Yang, Z. Chen, D.M. Shin, Application of nanotechnology in cancer therapy and imaging. CA Cancer J. Clin. **58**(2), 97–110 (2010)
2. K.M. Morrissey, T.M. Yuraszeck, C.-C. Li, Y. Zhang, S. Kasichayanula, Immunotherapy and novel combinations in oncology: current landscape, challenges, and opportunities. Clin. Transl. Sci. **9**(2), 89–104 (2016)
3. K.D. Miller, L. Nogueira, T. Devasia, A.B. Mariotto, K.R. Yabroff, A. Jemal, J. Kramer et al., Cancer treatment and survivorship statistics, 2022. CA Cancer J. Clin. **72**(5), 409–436 (2022)
4. T.J. Royce, M.M. Qureshi, M.T. Truong, Radiotherapy utilization and fractionation patterns during the first course of cancer treatment in the United States from 2004 to 2014. J. Am. Coll. Radiol. **15**(11), 1558–1564 (2018)
5. J.M. Brown, A.J. Giaccia, The unique physiology of solid tumors: opportunities (and problems) for cancer therapy. Can. Res. **58**(7), 1408–1416 (1998)
6. M. Das, C. Mohanty, Sanjeeb K Sahoo, Ligand-based targeted therapy for cancer tissue. Expert Opin. Drug Deliv. **6**(3), 285–304 (2009)
7. P. Mi, N. Nishiyama, Polymeric nanocarriers for cancer therapy, in *Nano-Oncologicals: New Targeting and Delivery Approaches*. ed. by B.M.H. Alonso, M. Garcia-Fuentes (Springer, Spain, 2014), pp.67–94
8. N.A. Atiyah, T.M. Albayati, M.A. Atiya, Functionalization of mesoporous MCM-41 for the delivery of curcumin as an anti-inflammatory therapy. Adv. Powder Technol. **33**(2), 103417 (2022)
9. N. Singh, S. Son, J. An, I. Kim, M. Choi, N. Kong, W. Tao, J.S. Kim, Nanoscale porous organic polymers for drug delivery and advanced cancer theranostics. Chem. Soc. Rev. **50**, 12883–12896 (2021)

10. S.B. Patil, S.Z. Inamdar, K.R. Reddy, A.V. Raghu, K.G. Akamanchi, A.C. Inamadar, K.K. Das, R.V. Kulkarni, Functionally tailored electro-sensitive poly (acrylamide)-g-pectin copolymer hydrogel for transdermal drug delivery application: synthesis, characterization, in-vitro and ex-vivo evaluation. Drug Deliv. Lett. **10**(3), 85–196 (2020)
11. S. Mohapatra, S. Ranjan, N. Dasgupta, R. Mishra, S. Thomas, *Nanocarriers carriers for drug delivery*, 1st edn. (Elsevier, Amsterdam, 2018)
12. M. Meyyappan, Nanotechnology: opportunities and challenges. Electron. Today **37**(9), 61–63 (2005)
13. P. Parhi, C. Mohanty, S.K. Sahoo, Nanotechnology-based combinational drug delivery: an emerging approach for cancer therapy. Drug Discovery Today **17**(17–18), 1044–1052 (2012)
14. J. Nicolas, L. Moine, G. Barratt, Polymeric nanoparticles for drug delivery, in *Polymeric Biomaterials*, 1st edn., ed. by S. Dumitriu, V. Popa (CRC Press, Florida, 2013), pp.123–152
15. A. Zielińska, F. Carreiró, A.M. Oliveira, A. Neves, B. Pires, D.N. Venkatesh et al., Polymeric nanoparticles: production, characterization Toxicology and Ecotoxicology. Molecules **25**(16), 3731 (2020)
16. S.Y. Lee, H.S. Park, K.Y. Lee, H.J. Kim, Y.J. Jeon, T.W. Jang et al., Paclitaxel-loaded polymeric micelle (230 mg/m(2)) and cisplatin (60 mg/m(2)) vs. paclitaxel (175 mg/m(2)) and cisplatin (60 mg/m(2)) in advanced non-small-cell lung cancer: a multicenter randomized phase iib trial. Clin. Lung Cancer **14**(3), 275–282 (2013)
17. S.W. Lee, Y.M. Kim, C.H. Cho, Y.T. Kim, S.M. Kim, S.Y. Hur et al., An open-label, randomized, parallel, phase ii trial to evaluate the efficacy and safety of a cremophor-free polymeric micelle formulation of paclitaxel as first-line treatment for ovarian cancer: a korean gynecologic oncology group study (KGOG-3021). Cancer Res. Treat. **50**(1), 195–203 (2018)
18. J.X. Zhang, M.Q. Yan, X.H. Li, L.Y. Qiu, X.D. Li, X.J. Li, Y. Jin et al., Local delivery of indomethacin to arthritis-bearing rats through polymeric micelles based on amphiphilic polyphosphazenes. Pharm. Res. **24**, 1944–1953 (2007)
19. X. Wang, Xu. Bing Wei, J.W. Cheng, R. Tang, Phenylboronic acid-decorated gelatin nanoparticles for enhanced tumor targeting and penetration. Nanotechnology **27**(38), 385101 (2016)
20. J.D. Twibanire, T.B. Grindley, Polyester dendrimers: smart carriers for drug delivery. Polymers **6**(1), 179–213 (2014)
21. X. Ke, V.W. Ng, R.J. Ono, J.M. Chan, S. Krishnamurthy, Y. Wang et al., Role of non-covalent and covalent interactions in cargo loading capacity and stability of polymeric micelles. J. control. Releas. **193**, 9–26 (2014)
22. T. Maeda, H. Otsuka, A. Takahara, Dynamic covalent polymers: reorganizable polymers with dynamic covalent bonds. Prog. Polym. Sci. **34**(7), 581–604 (2009)
23. P. Gou, W. Liu, W. Mao, J. Tang, Y. Shen, M. Sui, Self-assembling doxorubicin prodrug forming nanoparticles for cancer chemotherapy: synthesis and anticancer study in vitro and in vivo. J. Mater. Chem. B **1**(3), 284–292 (2013)
24. Y.E. Aguirre-Chagala, J.L. Santos, Y. Huang, M. Herrera-Alonso, Phenylboronic acid-installed polycarbonates for the ph-dependent release of diol-containing molecules. ACS Macro Lett. **3**(12), 1249–1253 (2014)
25. Hu. Xianglong, Hu. Jinming, J. Tian, Z. Ge, G. Zhang, K. Luo et al., Polyprodrug amphiphiles: hierarchical assemblies for shape-regulated cellular internalization, trafficking, and drug delivery. J. Am. Chem. Soc. **135**(46), 17617–17629 (2013)
26. A.C. Allison, R. Cacabelos, V.R. Lombardi, X.A. Alvarez, C. Vigo, Celastrol, a potent antioxidant and anti-inflammatory drug, as a possible treatment for Alzheimer's disease. Prog. Neuropsychopharmacol. Biol. Psychiatry **25**(7), 1341–1357 (2001)
27. A. Salminen, M. Lehtonen, T. Paimela, K. Kaarniranta, Celastrol: molecular targets of thunder god vine. Biochem. Biophys. Res. Commun. **394**(3), 439–442 (2010)
28. H. Zhu, W.-J. Ding, Wu. Rui, Q.-J. Weng, J.-S. Lou, R.-J. Jin, Synergistic anti-cancer activity by the combination of TRAIL/APO-2L and celastrol. Cancer Invest. **28**(1), 23–32 (2010)
29. S. Huang, Y. Tang, X. Cai, X. Peng, X. Liu, L. Zhang, Celastrol inhibits vasculogenesis by suppressing the VEGF-induced functional activity of bone barrow-derived endothelial progenitor cells. Biochem. Biophys. Res. Commun. **423**(3), 467–472 (2012)
30. S.Y. Jang, S.W. Jang, J. Ko, Celastrol inhibits the growth of estrogen positive human breast cancer cells through modulation of estrogen receptorα. Cancer Lett. **300**(1), 57–65 (2011)
31. P.-P. Li, W. He, P.-F. Yuan, S.-S. Song, Lu. Jing-Tao, W. Wei, Celastrol induces mitochondria-mediated apoptosis in hepatocellular carcinoma bel-7402 cells. Am. J. Chin. Med. **43**(1), 137–148 (2015)
32. H. Ni, W. Zhao, X. Kong, H. Li, J. Ouyang, Celastrol inhibits lipopolysaccharide-induced angiogenesis by suppressing tlr4-triggered nuclear factor-kappa B activation. Acta Haematol. **131**(2), 102–111 (2014)
33. V.R. Yadav, B. Sung, S. Prasad, R. Kannappan, S.G. Cho, M. Liu et al., Celastrol suppresses invasion of colon and pancreatic cancer cells through the downregulation of expression of CXCR4 chemokine receptor. J. Mol. Med. **88**(12), 1243–1253 (2010)
34. Y. Kim, H. Kang, S.-W. Jang, J. Ko, Celastrol inhibits breast cancer cell invasion via suppression of NF-κB-mediated matrix metalloproteinase-9 expression. Cell. Physiol. Biochem. **28**(2), 175–184 (2011)
35. X.H. Cai, J. Jin, M.H. He, 2016 Advances in structural modifications of celastrol. ARKIVOC **1**, 172–182 (2016)
36. A. Trott, J.D. West, L. Klaić, S.D. Westerheide, R.B. Silverman, R.I. Morimoto et al., Activation of heat shock and antioxidant responses by the natural product celastrol: transcriptional signatures of a thiol-targeted molecule. Mol. Biol. Cell **19**(3), 1104–1112 (2008)
37. J.H. Lee, T.H. Koo, H. Yoon, H.S. Jung, H.Z. Jin, K. Lee et al., Inhibition of NF-κB activation through targeting IκB kinase by celastrol, a quinone methide triterpenoid. Biochem. Pharmacol. **72**(10), 1311–1321 (2006)
38. S. Sreeramulu, S.L. Gande, M. Göbel, H. Schwalbe, Molecular mechanism of inhibition of the human protein complex Hsp90-Cdc37, a kinome chaperone-cochaperone, by triterpene celastrol. Angewandte chemie-international edition. **48**(32), 5853–5855 (2009)
39. P. Ashrit, B. Sadanandan, L. Kyathsandra Natraj, K. Shetty, V. Vaniyamparambath, A.V. Raghu, Microplate-based response surface methodology model for growth optimization and biofilm formation on polystyrene polymeric material in a Candida albicans and Escherichia coli co-culture. Polym. Adv. Technol. **33**(9), 2872–2885 (2022)
40. G. Divyashri, T.P. Murthy, K.V. Ragavan, G.M. Sumukh, L.S. Sudha, S. Nishka, G. Himanshi, N. Misriya, B. Sharada, R.A. Venkataramanaiah, Valorization of coffee bean processing waste for the sustainable extraction of biologically active pectin. Heliyon. **9**(9), e20212 (2023)
41. A.T. Khadim, T.M. Albayati, N.M. Saady, Removal of sulfur compounds from real diesel fuel employing the encapsulated mesoporous material adsorbent Co/MCM-41 in a fixed-bed column. Microporous Mesoporous Mat. **341**, 112020 (2022)
42. N.S. Ali, Z.T. Alismaeel, H.S. Majdi, H.G. Salih, M.A. Abdulrahman, N.M. Saady, T.M. Albayati, Modification of SBA-15 mesoporous silica as an active heterogeneous catalyst for the hydroisomerization and hydrocracking of n-heptane. Heliyon **8**(6), e09737 (2022)

43. N.S. Ali, N.M. Jabbar, S.M. Alardhi, H.S. Majdi, T.M. Albayati, Adsorption of methyl violet dye onto a prepared bio-adsorbent from date seeds: isotherm, kinetics, and thermodynamic studies. Heliyon. **8**(8), e10276 (2022)
44. A.V. Raghu, H.M. Jeong, J.H. Kim, Y.R. Lee, Y.B. Cho, K. Sirsalmath, Synthesis and characterization of novel polyurethanes based on 4-{(4-Hydroxyphenyl)iminomethyl}phenol. Macromol. Res. **16**(3), 194–199 (2008)
45. N.A. Atiyah, T.M. Albayati, M.A. Atiya, Interaction behavior of curcumin encapsulated onto functionalized SBA-15 as an efficient carrier and release in drug delivery. J. Mol. Struct. **1260**(15), 132879 (2022)
46. N.S. Ali, H.N. Harharah, I.K. Salih, N.M. Cata Saady, S. Zendehboudi, T.M. Albayati, Applying MCM-48 mesoporous material, equilibrium, isotherm, and mechanism for the effective adsorption of 4-nitroaniline from wastewater. Sci. Rep. **13**, 9837 (2023)
47. B. Salehi, Y. Berkay Yılmaz, G. Antika, T. Boyunegmez Tumer, M. Fawzi Mahomoodally, D. Lobine et al., Insights on the use of α-lipoic acid for therapeutic purposes. Biomolecules **9**(8), 356 (2019)
48. M. Foox, M. Zilberman, Drug delivery from gelatin-based systems. Expert Opin. Drug Deliv. **12**(9), 1547–1563 (2015)
49. Ş Yıldırım, H. Akyıldız, Z. Çetinkaya, Synthesis of glucose/fructose sensitive poly(ethylene glycol) methyl ether methacrylate particles with novel boronate ester bridge crosslinker and their dye release applications. Acta Chim. Slov. **69**(1), 39–48 (2022)
50. Wu. Zhongyu, M. Li, H. Fang, B. Wang, A new boronic acid based fluorescent reporter for catechol. Bioorg. Med. Chem. Lett. **22**(23), 7179–7182 (2012)
51. C. Wang, P. Qi, Lu. Yan, L. Liu, Y. Zhang, Q. Sheng et al., Bicomponent polymeric micelles for pH-controlled delivery of doxorubicin. Drug Deliv. **27**(1), 344–357 (2020)
52. P. Zhang, Xu. Qinan, X. Li, Y. Wang, pH-responsive polydopamine nanoparticles for photothermally promoted gene delivery. Mat. Sci. Eng. C Mater. Biol. Appl. **108**, 110396 (2020)
53. R. Mo, Gu. Zhen, Tumor microenvironment and intracellular signal-activated nanomaterials for anticancer drug delivery. Mater. Today **19**, 274–283 (2016)
54. A.A. Cluntun, M.J. Lukey, R.A. Cerione, J.W. Locasale, Glutamine metabolism in cancer: Understanding the heterogeneity. Trends Cancer. **3**(3), 169–180 (2017)
55. B. Sun, C. Luo, Yu. Han, X. Zhang, Q. Chen, W. Yang et al., Disulfide bond-driven oxidation- and reduction-responsive prodrug nanoassemblies for cancer therapy. Nano Lett. **18**(6), 3643–3650 (2018)
56. M.H. Lee, J.L. Sessler, J.S. Kim, Disulfide-based multifunctional conjugates for targeted theranostic drug delivery. Acc. chem. Res.. **48**(11), 2935–2946 (2015)
57. L. Zhang, Y. Ding, Q. Wen, C. Ni, Synthesis of core-crosslinked zwitterionic polymer nano aggregates and pH/Redox responsiveness in drug-controlled release. Mat. Sci. Eng. C Mater. Biol. Appl. **106**, 110288 (2020)
58. J. Qin, Y. Huang, G. Yan, J. Wang, Hu. Liefeng, P. Zhang, R. Tang, Phenylboronic acid-functionalized ultra-pH-sensitivemicelles for enhanced tumor penetration and inhibitionin vitro. J. Mater. Sci. **54**, 5695–5711 (2019)




## Authors and Affiliations

**Jiangtao Su[1,2,3,4] · Meng Rao[1] · Heshuang Dai[1,2] · Le Cai[1] · Fan Ye[1] · Lu Ye[1] · Yuchen Hu[1,3] · Ban Chen[1,4] · Xiaoxia Guo[1,2,3]**

✉ Xiaoxia Guo
20200031@hbut.edu.cn

[1] School of Biological Engineering and Food Science, Hubei University of Technology, No.28, Nanli Road, Wuhan 430068, China

[2] National '111' Center for Cellular Regulation and Molecular Pharmaceutics, Hubei University of Technology, Wuhan 430068, China

[3] Key Laboratory of Industrial Microbiology in Hubei, Hubei University of Technology, Wuhan 430068, China

[4] Hubei Province Cooperative Innovation Center for Industrial Fermentation, Hubei University of Technology, Wuhan 430068, China